PHYSICAL REVIEW E **80**, 011310 (2009)

Magnetically driven surface mixing

M. Belkin,[1,2] A. Snezhko,[1] I. S. Aranson,[1] and W.-K. Kwok[1]

[1]*Materials Science Division, Argonne National Laboratory, 9700 South Cass Avenue, Argonne, Illinois 60439, USA*

[2]*Illinois Institute of Technology, 3101 South Dearborn Street, Chicago, Illinois 60616, USA*

(Received 20 April 2009; published 28 July 2009)

Magnetic microparticles suspended on the surface of liquid and energized by vertical alternating magnetic field exhibit complex collective behavior. Various immobile and self-propelled self-assembled structures have been observed. Here, we report on experimental studies of mixing and surface diffusion processes in this system. We show that the pattern-induced surface flows have properties of quasi-two-dimensional turbulence. Correspondingly, the surface advection of tracer particle exhibits properties of Brownian diffusion.

DOI: 10.1103/PhysRevE.80.011310 PACS number(s): 45.70.−n, 87.19.ru, 47.63.Gd, 75.50.Tt

Fundamental mechanisms governing collective behavior and self-organization in nonequilibrium systems with complex interactions continue to attract significant attention in the scientific community. There is a large number of theoretical and experimental works focused on collective behavior in a broad class of systems spanning from granular materials [1–9] to suspensions of live bacteria [10–13]. Although these systems have obvious fundamental differences in the specific interaction mechanisms between the elements, the manifestation of collective behavior often shows a certain degree of similarity.

Recent studies of complex collective behavior in systems of magnetic microparticles suspended on a liquid-air interface brought to light a new intriguing phenomenon—dynamic self-assembled magnetic structures—called magnetic "snakes" [14–17] due to their eye-catching similarity to living snakes. It was demonstrated [16] that each snake was accompanied by four large-scale hydrodynamic vortices induced on the surface of the liquid (vortex quadrupole). The strength of the vortices can be effectively tuned by the frequency and amplitude of the external magnetic field. Further investigation revealed that the snakes demonstrate additional (secondary) instability with respect to self-induced surface flows: at increased driving frequencies the snakes may spontaneously break the symmetry of the surface flows and turn into self-propelled entities [18]. The number of swimming snakes increases with the number of magnetic particles on the surface of fluid. In such a multiple-snake state all the snakes strongly interact with each other by means of surface flows, creating a nonperiodic recurring motion on the liquid surface. One anticipates that the interplay of these nonsteady flows generated by multiple interacting snakes will effectively mix the surface of the liquid.

In this paper, we characterize the mixing properties of the multiple-snake state. We demonstrate that the flow dynamics induced by moving snakes has a signature of quasi-two-dimensional turbulence: the power spectrum of the velocity fluctuations shows a power-law behavior. Consequently, a passive tracer diffusion in such a pattern-assisted velocity field shows properties of conventual two-dimensional Brownian motion.

Our experiments were conducted on 90 μm nickel spherical particles suspended on the surface of water and supported by the latter's surface tension. Our experimental setup is similar to that used in Ref. [15]. A glass container (7 cm in diameter) containing particles suspended on water (5 cm depth) is placed in the center of a pair of magnetic Helmholtz coils capable of generating a vertical magnetic field of up to 170 Oe. An alternating magnetic field is used to energize the system. The trajectories of the microparticles are monitored by a fast charge-coupled device camera mounted above the container on top of an optical microscope stage. The acquired images are then processed using a particle image velocimetry (PIV) technique in order to extract the velocity fields of the surface flow dynamics. In most of our earlier experiments [15,17] the number of microparticles suspended on the surface of the liquid and the range of parameters of the external magnetic field were selected to guaranty a formation of a self-assembled single snake structure. While a single snake produces rather fast large-scale surface flows at its ends, the snake itself typically remains immobile due to the balanced symmetry of self-generated flows at the ends of the snake. Increase in the number of particles and/or the frequency of external magnetic field promotes a formation of multiple snakes which are in turn unstable with respect to self-induced flows and become mobile swimmers [18]. These magnetic swimmers are self-propelled due to a spontaneously developed intrinsic asymmetry of their vortex flows. The snakes swim erratically and actively interact with other snakes in the container, resulting in a highly disordered and nonperiodic structure of the surface velocity field. Figure 1 illustrates a typical velocity field in the regime of multiple swimmers. Remarkably, whereas some snakes swim, other snakes may temporary rest in the vicinity of the container's wall, with their tails actively wiggling from side to side. Eventually, a swimmer may come by and either adsorb or destroy them. Both processes lead to a rather rapid transport of tracer particles and stirring at the surface of fluid; see movie [19]. The rate of this chaotic mixing and the possibility to control it by means of an applied magnetic field is an interesting and nontrivial issue. Our system demonstrates recurrent evolution of these dynamic snakelike structures which are self-assembled and annihilated in a succession over several seconds. To characterize an effective mixing rate related to the averaged kinetic energy fluctuations of the fluid (or "effective temperature") in this system, we introduce a rms velocity of the surface flows. While instantaneous values of the rms velocity fluctuate (being dependent on the number and configuration of snakes), averaged over time and space values provide adequate characterization of the dy-

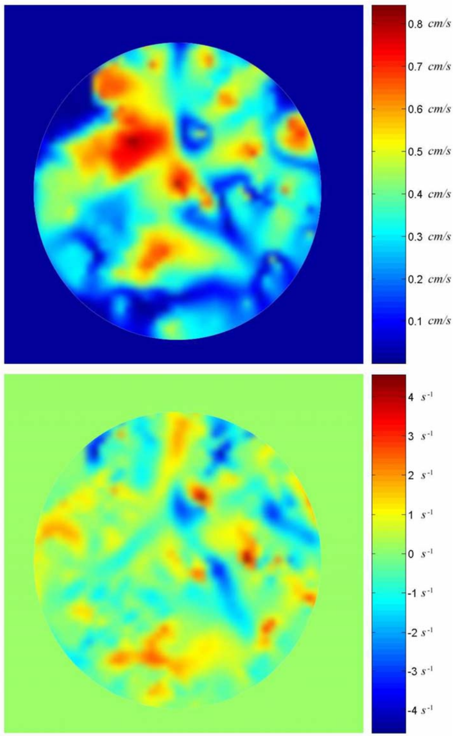

FIG. 1. (Color online) Top picture: snapshot of typical velocity field induced by the dynamic multisnake pattern. Bottom picture: snapshot of a typical vorticity field generated by the dynamic pattern at the interface.

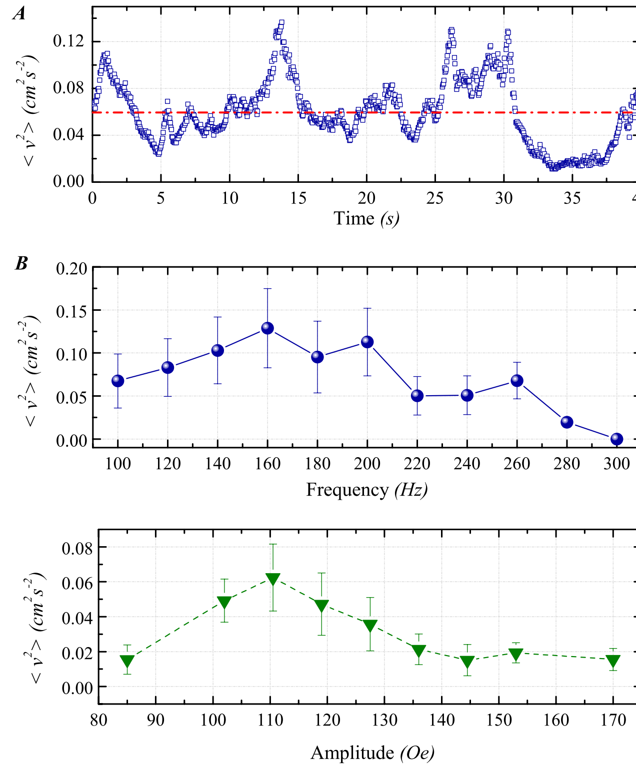

FIG. 2. (Color online) Root mean square (rms) velocity of the surface flows. Panel A: typical evolution of rms velocity during one experiment. Panel B: dependence of rms velocity on the frequency and amplitude of applied magnetic field. Amplitude dependence was studied at $f_0 = 100$ Hz; frequency dependence was examined at $H_0 = 119$ Oe.

namic state. Figure 2 (panel A) depicts typical behavior of the rms velocity plotted as a function of time. Apparently, it is sensitive to the parameters of the external excitations (frequency and amplitude of applied magnetic field). Corresponding dependencies are shown in Fig. 2 (panel B). Indeed, one can see broad peaks in the rms velocity of the system at amplitudes around 110 Oe and frequencies of about 160 Hz. There is a simple explanation for the origin of these peaks: exciting the system with low frequency and/or amplitude does not supply enough energy, whereas at too high frequencies the magnetic particles stop responding to the applied field due to their inertia. Moreover, at too strong ac magnetic fields the particles prefer to form a triangular lattice (with the dipole moments of particles oriented along the field direction) resulting in nonzero but significantly suppressed diffusion. Thus, there is an intermediate range of driving parameters where excitation of surface flows by external periodic excitation of particles is the most efficient. Apparently, this range coincides with the one of existence of dynamic self-assembled snake patterns and strongly depends on the magnetic properties of the particles involved in self-assembly: increased magnetic moment per particle would shift up the amplitude and frequency ranges of the external driving field used to generate our snake patterns (see Refs. [8,15]).

To further characterize the mixing properties in our system we study the diffusion of passive nonmagnetic tracers on the surface of the liquid. As a tracer we use a light-weight glass bead of about 0.5 mm in diameter. In contrast to our previous experiments where a large bead was used to suppress one of the vortex pairs of the snake, the present smaller and lighter particle introduces only a small perturbation to the flow dynamics.

Typical trajectories of the tracer are shown in the top panel of Fig. 3. The position of the tracer is tracked in each frame of the acquired image sequences and the mean square displacement, r_i, of the tracer was extracted from the data. Particle's diffusion coefficient D was defined as following:

$$\langle \mathbf{r}^2 \rangle = 4Dt, \tag{1}$$

where t is time. The Brownian character of the tracer's motion can be illustrated by the radial probability density function, which for a two-dimensional diffusion process is given by

$$P(r,t) \sim r \exp\left(-\frac{r^2}{4Dt}\right). \tag{2}$$

Panel B in Fig. 3 shows the radial probability density $P(r)$ at time $t = 1.2$ s. A fit to Eq. (2) agrees closely with the obtained experimental data, providing a clear evidence for Brownian-type motion of the tracer. Alternatively, the diffusion coefficient D can be extracted from the mean square displacements of the tracer positions. Figure 4 (panel A) shows the typical dependence of the mean square displacement of the tracer particle as a function of time. The diffusion coefficient is in a

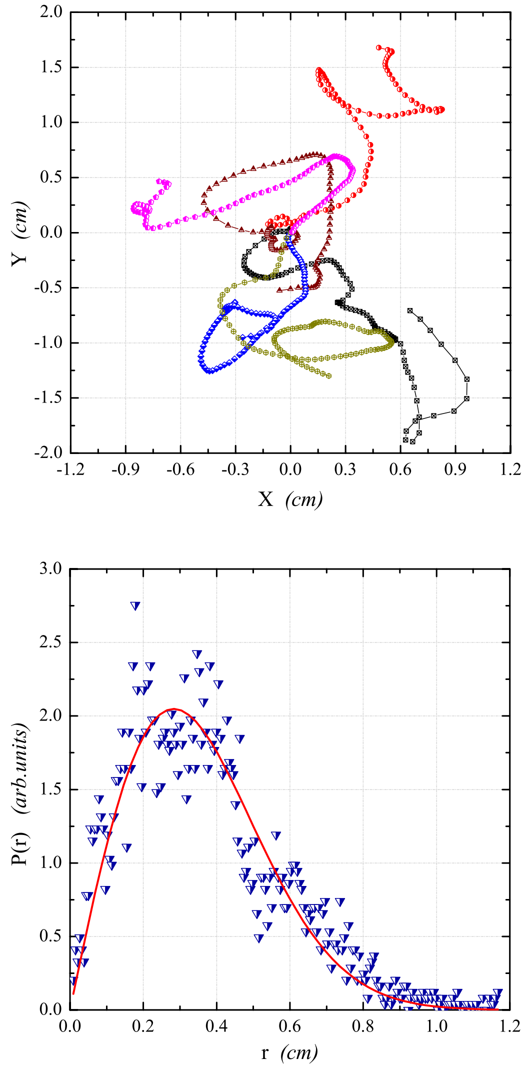

FIG. 3. (Color online) Top panel: typical examples of tracer particle trajectories. Starting positions has been moved to the origin. Bottom panel: radial probability density $P(r)$ of a tracer at $t=1.2$ s. $H_0=120$ Oe, $f_0=150$ Hz. Solid line is the best fit to Eq. (2). Diffusion coefficient extracted from the fit, $D=0.033$ cm^2 s^{-1}.

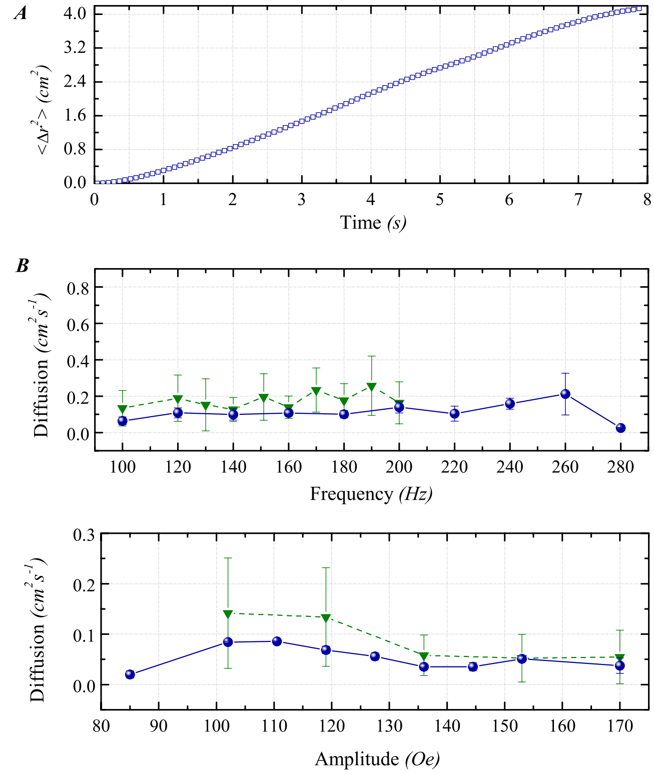

FIG. 4. (Color online) Panel A: mean square displacement as a function of time. Panel B: dependence of the diffusion coefficient D on the frequency and amplitude of applied magnetic field. Amplitude dependence was examined at $f_0=100$ Hz; the frequency dependence was studied at $H_0=119$ Oe. Curves extracted from the analysis of mean square displacement of a passive tracer are shown with triangles. Curves obtained by examining temporal autocorrelation functions of the surface velocity field are shown with circles.

good agreement with that extracted from the fit to a radial probability density function. To investigate the dependence of the diffusion coefficient D on the parameters of applied magnetic field, the above procedures have been carried out for different values of amplitudes and frequencies of the magnetic field; the results are presented in Fig. 4 (panel B). One sees that the diffusion coefficient is roughly a constant over a broad range of the applied magnetic field parameters. Certainly, one should keep in mind that this kind of behavior exists only in the range of parameters where swimming snakes are present in our system. Further increase in the frequency or amplitude of applied magnetic field affects the process of self-assembly itself: particles stop reacting on alternating magnetic field above 300 Hz. On the other hand, too high amplitude of the magnetic field destroys snakes and produces just a regular triangular lattice of magnetic particles on the surface. Apparently, as one approaches the region of excitation parameters where dynamic self-assembled snakes are not favorable, a decrease in the diffusion coefficient is observed with a subsequent suppression of the diffusion.

Additional information on statistical and transport properties of our system was obtained from the analysis of spatial and temporal velocity correlation functions of the surface flows. To calculate the correlation functions, we first extracted the surface flow velocity fields by the means of particle image velocimetry [20] for different parameters of the applied field. We used the same nickel particles as tracers on the surface that were not incorporated into the snake structures. While these tracers are not completely passive (since they interact with the external driving field) they still provide a rather good characterization of the surface flows. A typical spatial correlation function is presented in Fig. 5 (panel A). It has pronounced oscillations around zero; this feature is common for spatial correlations in the presence of large-scale vortex structures in the system. Indeed, due to the vortices, the velocity's directions are well correlated resulting in a negative contribution to the correlation coefficient. As the correlation length we selected the position of the first observable bump on the spatial correlation curve. As depicted in Fig. 5 (panel B), variations in the amplitude and frequency of the external magnetic field produce almost no effect on the spatial correlation length of the system (the same trends are

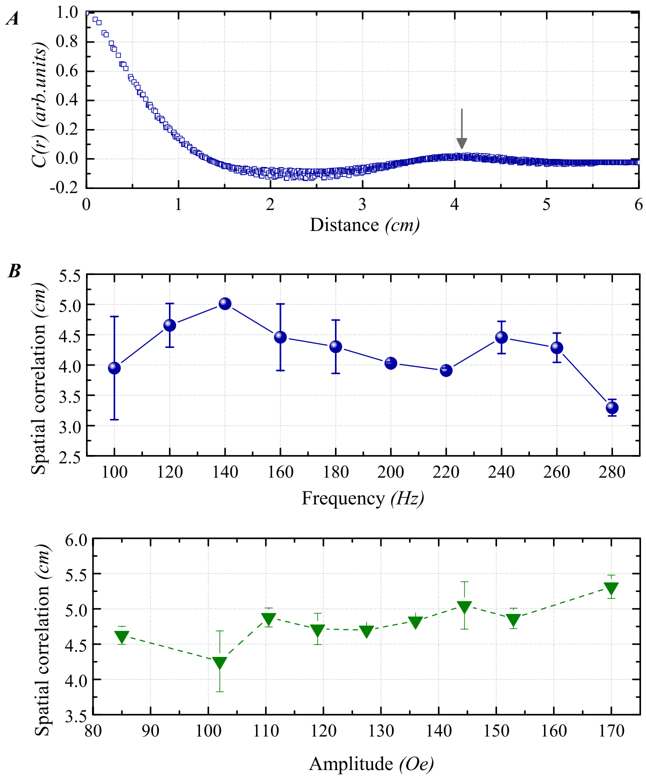

FIG. 5. (Color online) Panel A: spatial velocity correlation function ($H_0=145$ Oe, $f_0=100$ Hz). Panel B: dependence of the correlation length on the frequency and amplitude of applied magnetic field. Arrow indicates position of the first bump on correlation function. Amplitude dependence was examined at $f_0=100$ Hz; frequency dependence was examined at $H_0=119$ Oe.

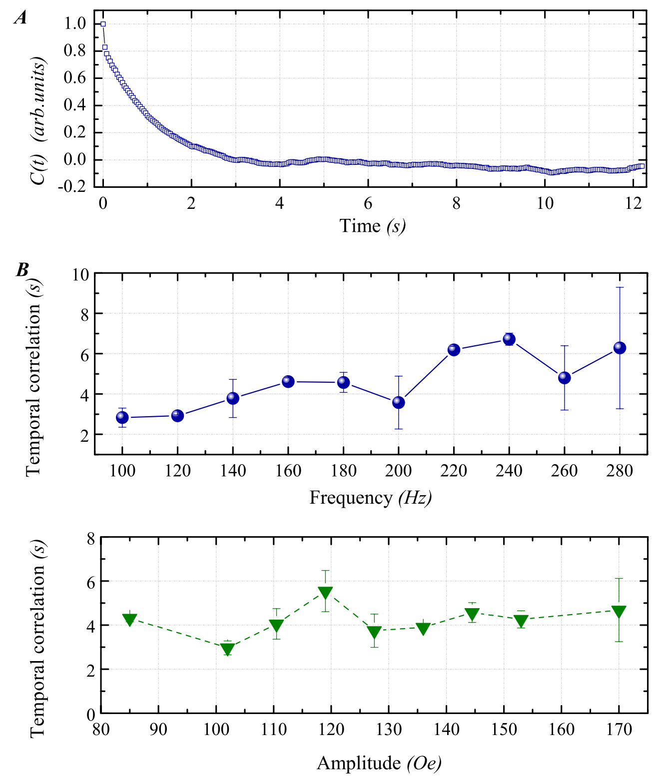

FIG. 6. (Color online) Panel A: temporal velocity correlation function ($H_0=119$ Oe, $f_0=120$ Hz). Panel B: correlation time as a function of frequency and amplitude of external magnetic field. Amplitude dependence was studied at $f_0=100$ Hz; frequency dependence was examined at $H_0=119$ Oe.

observed when one selects the position of first zero in the correlation curve as the correlation length). In order to extract the dependence of correlation time on the amplitude and frequency of the applied magnetic field, we performed several experiments, each producing around 3600 curves for every value of frequency or amplitude. A typical temporal correlation function is depicted in Fig. 6 (panel A). The temporal correlation function provides an alternative way to estimate the diffusion coefficient. For a two-dimensional motion, the diffusion coefficient can be calculated as

$$D = \frac{1}{2}\int_{t_0}^{\infty} \langle v(t')v(t_0)\rangle dt' . \quad (3)$$

Here, the integrand is an autocorrelation function of the velocity field. Diffusion coefficients extracted from the correlation functions are presented in Fig. 4 (panel B). The resulting curves are close to those previously obtained from the tracking of the passive tracer. However, the diffusion values extracted from the tracer positions are typically slightly higher than that obtained from the correlation functions. We believe that this discrepancy is due to the fact that nickel particles used in the PIV analysis are not perfectly passive tracers: their magnetic interactions slightly reduce the actual value of the measured velocity field.

Correlation analysis also allows us to investigate the energy spectrum of turbulent fluctuations in our system. Since the characteristic Reynolds number associated with the motion of snakes, Re ~ 500–1000, is not very high, we expect that the hydrodynamic turbulence in our system should not be well developed. Nevertheless, we extracted the Kolmog-

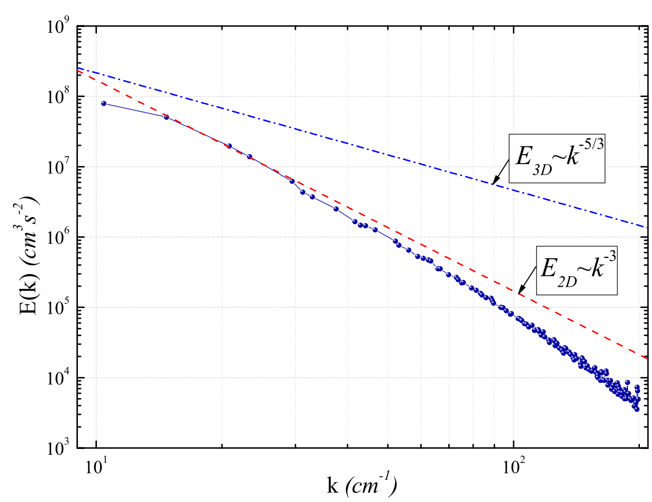

FIG. 7. (Color online) Typical energy spectrum of the surface flows ($f_0=100$ Hz, $H_0=119$ Oe). The dashed line shows fit to two-dimensional Kolmogorov law $E(k)\propto k^{-3}$. Energy spectrum of a three-dimensional turbulence: $E(k)\propto k^{-5/3}$ (dashed-dotted line).

orov energy spectra $E(k)$ (energy density E per unit wave number k) from our experimental data. An example of the energy spectrum curve in logarithmic scales is shown in Fig. 7. Although the size constrains of our system limit the values of wave number k to only one decade, an approximate power-law behavior can be observed. Our results show that the scaling of the energy spectra is consistent with the behavior of a two-dimensional well-developed isotropic turbulence $E(k) \propto k^{-3}$ [21] yielding an exponent slightly smaller than 3. Thus, although our system is formally three dimensions (the depth of the container is comparable to the container's diameter), these results indicate that the stirring of the water's surface by swimming snakes is essentially a two-dimensional phenomenon, i.e., the flows are localized near the surface.

To conclude, we conducted studies of mixing and tracer diffusion processes in a system of driven magnetic particles at the water-air interface. The diffusion coefficients in the regimes of multiple self-assembled swimmers were extracted independently from the analysis of mean square displacement of passive tracers and by examining the temporal autocorrelation functions of surface flows. Both methods yield similar results.

We also established that pattern-induced surface flows demonstrate properties of a quasi-two-dimensional turbulence despite the fact that the geometry of our experiment is three dimensional one.

Our studies provide important clues related to the mixing properties at the air-water interface and more generally at the interface of two immiscible fluid interfaces (e.g., oil-water) perturbed by magnetic particles. One may think of a possible application of our studies for a noncontact interfacial stirring for compact chemical reactors and mixers.

This research was supported by U.S. DOE (Contract No. DE-AC02-06CH11357).

[1] M. C. Cross and P. C. Hohenberg, Rev. Mod. Phys. **65**, 851 (1993).
[2] I. S. Aranson and L. S. Tsimring, Rev. Mod. Phys. **78**, 641 (2006).
[3] P. Umbanhowar, F. Melo, and H. L. Swinney, Nature (London) **382**, 793 (1996).
[4] W. Losert, L. Bocquet, T. C. Lubensky, and J. P. Gollub, Phys. Rev. Lett. **85**, 1428 (2000).
[5] C. S. Orellana, I. S. Aranson, W.-K. Kwok, and S. Rica, Phys. Rev. E **72**, 040301(R) (2005).
[6] M. V. Sapozhnikov, Y. V. Tolmachev, I. S. Aranson, and W.-K. Kwok, Phys. Rev. Lett. **90**, 114301 (2003).
[7] E. Clement, L. Vanel, J. Rajchenbach, and J. Duran, Phys. Rev. E **53**, 2972 (1996).
[8] A. Snezhko, I. S. Aranson, and W.-K. Kwok, Phys. Rev. Lett. **94**, 108002 (2005).
[9] A. Kudrolli, G. Lumay, D. Volfson, and L. S. Tsimring, Phys. Rev. Lett. **100**, 058001 (2008).
[10] J. P. Hernandez-Ortiz, C. G. Stoltz, and M. D. Graham, Phys. Rev. Lett. **95**, 204501 (2005).
[11] C. Dombrowski, L. Cisneros, S. Chatkaew, R. E. Goldstein, and J. O. Kessler, Phys. Rev. Lett. **93**, 098103 (2004).
[12] A. Sokolov, I. S. Aranson, J. O. Kessler, and R. E. Goldstein, Phys. Rev. Lett. **98**, 158102 (2007).
[13] B. M. Haines, I. S. Aranson, L. Berlyand, and D. A. Karpeev, Phys. Biol. **5**, 046003 (2008).
[14] A. Snezhko, I. S. Aranson, and W.-K. Kwok, Phys. Rev. Lett. **96**, 078701 (2006).
[15] A. Snezhko, I. S. Aranson, and W.-K. Kwok, Phys. Rev. E **73**, 041306 (2006).
[16] M. Belkin, A. Snezhko, I. S. Aranson, and W.-K. Kwok, Phys. Rev. Lett. **99**, 158301 (2007).
[17] A. Snezhko and I. S. Aranson, Phys. Lett. A **363**, 337 (2007).
[18] A. Snezhko, M. Belkin, I. S. Aranson, and W.-K. Kwok, Phys. Rev. Lett. **102**, 118103 (2009).
[19] See EPAPS Document No. E-PLEEE8-80-117907 for movie illustrating mixing process by multiple erratically moving snakes at the surface of liquid. For more information on EPAPS, see http://www.aip.org/pubservs/epaps.html.
[20] J. K. Sveen, MATPIV, Version 1.6.1, Department of Mathematics, University of Oslo, 2004.
[21] V. E. Zhakharov, V. S. L'vov, and G. Falkovich, *Kolmogorov Spectra of Turbulence: Wave Turbulence*, Springer Series in Nonlinear Dynamics (Springer-Verlag, Berlin, 1992), Vol. 1.